Influence of nanocrystal distribution on electroluminescence from Si+-implanted SiO2 thin films

Ding, Liang; Chen, Tupei; Yang, Ming; Zhu, Fu Rong

2008

Ding, L., Chen, T., Yang, M., & Zhu, F. R. (2008). Influence of nanocrystal distribution on electroluminescence from Si+-implanted SiO2 thin films. Silicon photonics III.

https://hdl.handle.net/10356/93791

https://doi.org/10.1117/12.762617

Influence of nanocrystal distribution on electroluminescence from Si^+-implanted SiO_2 thin films

L. Ding*[a], T. P. Chen[a], M. Yang[a], and F. R. Zhu[b]
[a]School of Electrical and Electronic Engineering, Nanyang Technological University, Singapore 639798; [b]Institute of Materials Research and Engineering, Singapore 117602

ABSTRACT

Light emitting diodes (LEDs) based on a metal-oxide-semiconductor-like (MOS-like) structure with Si nanocrystals (*nc*-Si) embedded in SiO_2 have been fabricated with low-energy ion implantation. Under a negative gate voltage as low as ~-5 V, both visible and infrared (IR) electroluminescence (EL) have been observed at room temperature. The EL spectra are found to consist of four Gaussian-shaped luminescence bands with their peak wavelengths at ~460, ~600, ~740, and ~1260 nm, in which the ~600-nm band dominants the spectra. The EL properties have been investigated together with the current transport properties of the Si^+-implanted SiO_2 films. A systematic study has been carried out on the effect of the Si ion implantation dose and the energy on both the current transport and EL properties. The mechanisms of the origin of the four different EL bands have been proposed and discussed.

Keywords: electroluminescence, nanocrystals, implantation

1. INTRODUCTION

Over the past decade, intensive research has been carried out on the development of optoelectronic devices that are compatible with the mainstream complementary metal-oxide-semiconductor (CMOS) technology in the semiconductor industry.[1-9] As well known, most of the photonic components fabricated with Si technology have been demonstrated, such as optical modulators,[1,2] switches,[3,4] low-loss waveguides,[5,6] and detectors.[7,8] The observation of photoluminescence (PL) from porous Si at room temperature has attracted much research attention to fabricate Si-based light emitting devices employing low dimensional Si materials, in which the quantum confinement effect was initially thought to be the main mechanism of the strong luminescence.[9] A lot of efforts based on various techniques have been made to synthesize low dimensional Si, preferably Si nanocrystals (*nc*-Si). Among all these techniques, Si ion implantation into SiO_2 films followed by high temperature annealing has received the most intensive interest with the advantage of being fully compatible with mainstream Si technology and allowing for introduction of chemically and electrically stable *nc*-Si in robust dielectrics.[10-29]

Strong photoluminescence in the range from red to blue has been observed from Si^+-implanted SiO_2 films by a lot of research groups although the mechanism of the luminescence is not exclusively attributed to the quantum confinement effect of the *nc*-Si embedded in SiO_2.[10-18, 21-25] Recently, visible electroluminescence from Si^+-implanted SiO_2 films has also been demonstrated.[16-18, 22-24] Even a possibility of electrically driven ultraviolet light emission from Si^+-implanted SiO_2 films was predicted.[22] In the most studies focused on the luminescence properties of the *nc*-Si embedded in an oxide matrix, the authors employed silica glass or SiO_2 films as thick as hundreds of nanometers.[10-24] The thick oxide films are not suitable to fabricate efficient light emitting devices, because a higher oxide thickness indicates a poorer carrier injection. In practical, in order to achieve efficient carrier injection into the Si^+-implanted layers and make EL intensity strong enough, SiO_2 thin films less than 100 nm must be employed as the base material for Si ion implantation. Furthermore, almost all the researchers investigating on the EL properties of Si^+-implanted SiO_2 films used medium- or high-energy ion implantation. However, little investigation has been carried out on the EL properties of SiO_2 films embedded with *nc*-Si synthesized with low-energy ion implantation. [10-24] It is more practicable and inexpensive to use low-energy ion implantation to synthesize *nc*-Si embedded in SiO_2 films with most CMOS fabrication facilities. In this paper, we have systemically studied the EL together with the current transport properties of thin SiO_2 films embedded with *nc*-Si fabricated with low-energy ion implantation. The influence of nanocrystal distribution on the EL properties as well as the current transport of the Si^+-implanted SiO_2 films have been investigated in order to provide more information for the realization of CMOS-compatible light emitting devices.

*ding0008@ntu.edu.sg

Silicon Photonics III, edited by Joel A. Kubby, Graham T. Reed
Proc. of SPIE Vol. 6898, 68980H, (2008) · 0277-786X/08/$18 · doi: 10.1117/12.762617

2. EXPERIMENTS

SiO_2 films as thin as 30 nm were thermally grown on *p*-type Si wafers with (100) orientation at 950 ^oC in dry oxygen. Various doses of Si ions were implanted into the SiO_2 films at different implantation energies. For the study of influence of different doses, three samples were fabricated with the Si ion dose of 1×10^{16}, 2×10^{15}, and 3×10^{14} cm^{-2} at the energy of 5 keV; for the study of the influence of implantation energies, another three samples were fabricated with the Si ion dose of 1×10^{16} ions/cm^2 at the energy of 8 keV, 5 keV, and 2 keV, respectively. Table 1 summaries the implantation recipes of the samples under investigation, and each sample is denoted with a sample number. After implantation, thermal annealing was carried out at 1000 ^oC in N_2 ambient for 1 h to induce nanocrystallzation of excess Si atoms in SiO_2. Afterwards, the backside of the wafer was coated with a layer of Al as the back ohmic contact with the thickness of about 1 μm after the removing the native oxide. Finally, a 130-nm-thick layer of indium tin oxide (ITO) was deposited onto the surface of the Si^+-implanted SiO_2 film with a pad radius of 1.2 mm. The ITO layer has a sheet resistance of 25 Ω/sq and an average transmittance of 85% over the visible to infrared range. Detail of the ITO deposition and characterization can be found in previous studies.[30-32] The ITO film serves as a semitransparent gate electrode and the EL emission window. The cross-sectional transmission electron microscopy (TEM) image confirms the formation of *nc*-Si embedded in the SiO_2 matrix. As an example, Figure 1 shows the TEM images of *nc*-Si with the size of ~-4 nm embedded in the SiO_2 matrix for sample 8a. The implanted Si depth profiles in the SiO_2 films were calculated with Stopping and Range of Ions in Matter (SRIM) simulations. Figure 2 shows the depth profiles of excess Si calculated with SRIM simulations for the 5 samples. As can be seen in Fig. 2(a), for the samples implanted at 5 keV, the excess Si distributes from the oxide surface to the depth of ~23 nm, and the concentration of excess Si reaches its maximum at the depth of ~8 nm. The peak concentrations of excess Si for sample 5a, 5b, and 5c are 1×10^{22} cm^{-3}, 2×10^{21} cm^{-3}, and 3×10^{20} cm^{-3}, respectively. The corresponding peak *nc*-Si volume fractions are 20%, 4%, and 0.6%. The depth profiles of excess Si for the samples fabricated with different implanted energies but the same dose (i.e. sample 8a, 5a, and 2a) are presented in Fig. 2(b). As shown in this figure, for sample 8a, the excess Si distributes throughout the entire oxide region with the peak concentration of 5.7×10^{22} cm^{-3} (with the corresponding *nc*-Si volume fraction of 11%) located at the depth of ~15 nm from the oxide surface. For sample 2a, the excess Si distributes to the depth of ~15 nm and reaches its maximum of 1.7×10^{22} cm^{-3} (with the corresponding volume fraction of 33% or *nc*-Si) at the depth of ~4.5 nm. The current-voltage (*I-V*) and measurements for the light emitting structures were conducted with a HP4156A semiconductor characterization system. The EL measurements were carried out with a PDS-1 photomultiplier tube detector connected with a monochromator. All measurements were performed at room temperature.

Table 1. Summarization of implantation recipes for different samples

Sample No.	Implantation energy (keV)	Si ion dose (cm^{-2})
5a	5	1×10^{16}
5b	5	2×10^{15}
5c	5	3×10^{14}
8a	8	1×10^{16}
2a	2	1×10^{16}

3. RESULTS

Figure 3 shows the current-voltage (*I-V*) characteristics of the LED structure for all the samples listed in Table 1. Note that the *I-V* characteristics are presented by the relationship between gate current density (J_g) and gate voltage (V_g). It has been found that the *I-V* characteristics for all the samples follow a power law. The power law fittings are also presented for comparison in Fig. 3. As can be seen in Fig. 3(a), J_g increases with the implanted Si dose. The conduction enhancement with the increasing implanted Si ion dose can be explained with the current conduction model for the SiO_2 film distributed with *nc*-Si proposed in Ref. [33]. Electron tunneling can take place between adjacent neutral nanocrystals, and many such nanocrystals form conduction paths in the *nc*-Si embedded oxide region. Therefore, it is not surprising that the gate current density increases with *nc*-Si concentration, which can be attributed to the formation of more tunneling paths. As can be seen in Fig. 3(b), the gate current density increases with the implantation energy. This can also be explained by the *nc*-Si-related tunneling path model. As shown in Fig. 2(b), one can see that the *nc*-Si distributes throughout the entire oxide for sample 8a and partially distributes in the oxide for sample 5a and 2a. With the

reducing implantation energy, the *nc*-Si distribution region becomes narrower, thus lead to shorter tunneling path formed by *nc*-Si. Therefore, the remaining pure SiO_2 thickness is higher for the sample with lower implantation energy. The remaining pure SiO_2 plays the most important role in the whole film resistance. This explains why the gate current decreases when reducing implantation energy.

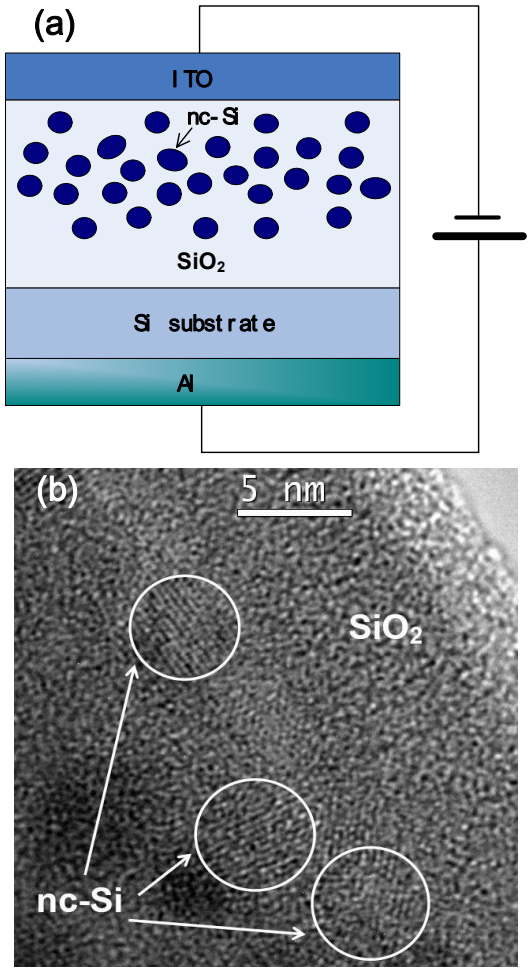

Fig. 1. (a) Schematic illustration of the LED structure. (b) Cross-sectional TEM image of *nc*-Si embedded in SiO_2 for sample 8a.

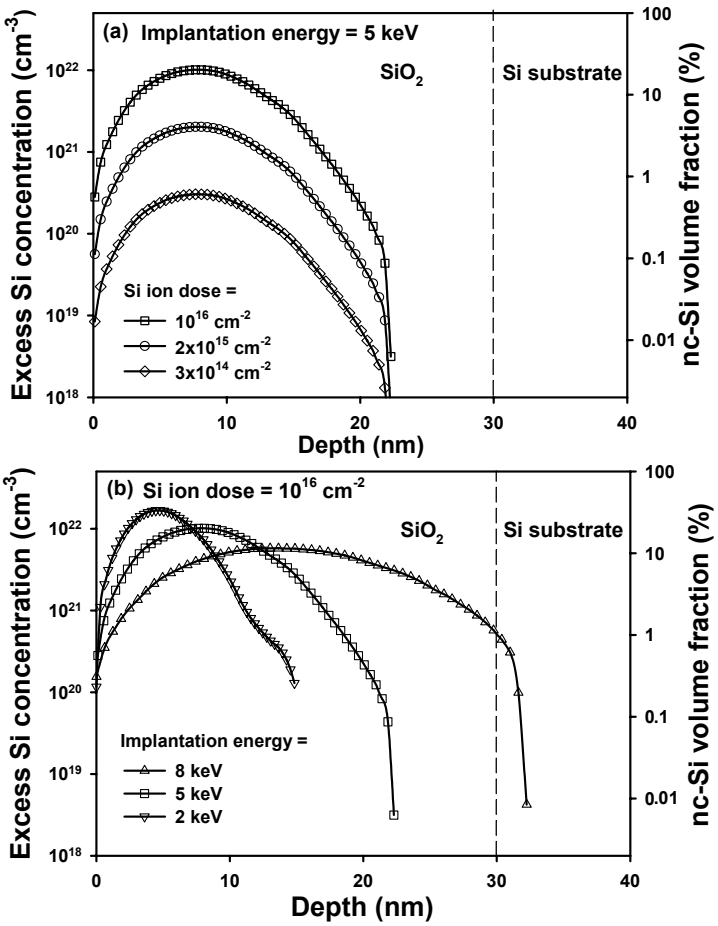

Fig. 2. Distribution of nc-Si in the gate oxide calculated from SRIM simulation.

Visible and infrared electroluminescence can be observed from our MOS-like LED structures when a negative gate voltage is applied. No electroluminescence was detected under a positive gate voltage due to the extremely low gate current. When a positive gate voltage is applied, the holes can hardly be provided by the ITO contact, and the electrons are minorities in *p*-type Si substrate. Therefore, a strong EL is difficult to be induced under a positive gate voltage due to the extremely low injection of holes from the positively biased ITO gate and electrons from *p*-type Si substrate. As a typical investigation, Fig. 4(a) shows the EL spectra for sample 5a under different gave voltages. As shown in this figure, one can see that the EL intensity increases with the applied gate voltage, but the spectral shape change little under different gate voltages. Figure 4(b) shows *I-V* characteristics as well as the integrated EL intensity versus gate voltage for sample 5a. The integrated EL intensity was obtained as an average value measured from several LEDs on sample 5a, and the error bars are given to ensure the accuracy. As can be seen in Fig. 4(a), the integrated EL intensity varies with gate voltage in a way similar to the gate current density, indicating a linear relationship between the integrated EL intensity and the current density.

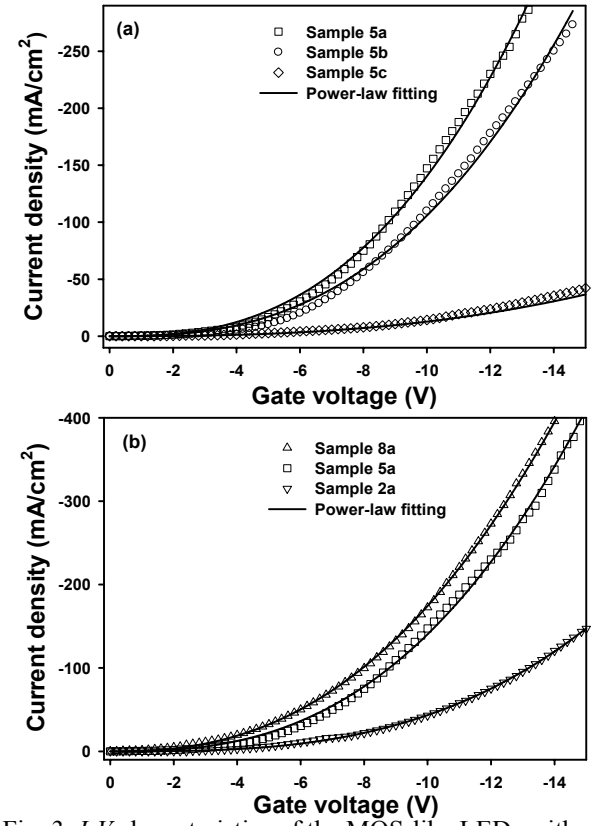

Fig. 3. *I-V* characteristics of the MOS-like LEDs with nc-Si distributed in the oxide.

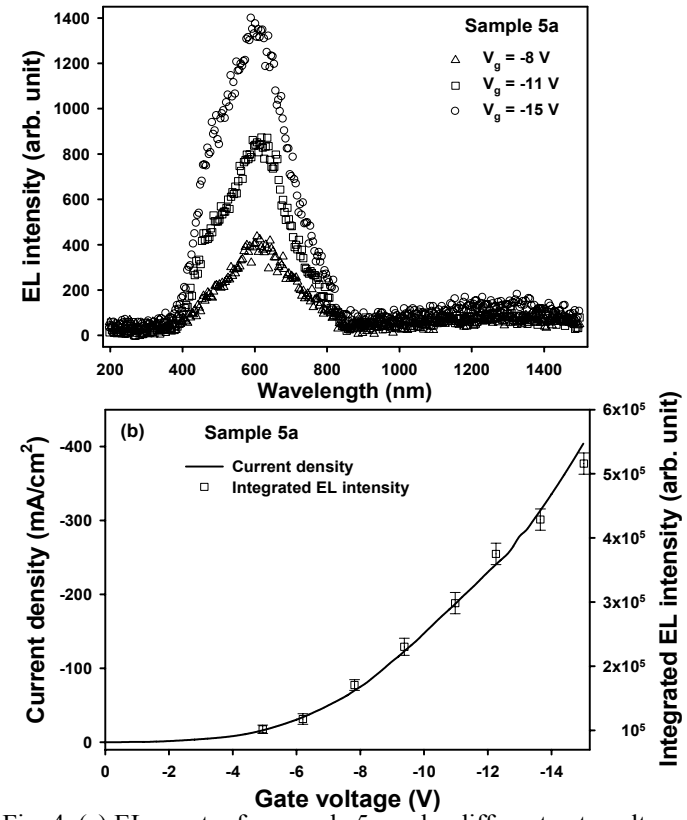

Fig. 4. (a) EL spectra for sample 5a under different gate voltages; (b) Dependences of the current density and of the integrated EL intensity on the applied gate voltage for sample 5a.

The EL spectra can be decomposed into four Gaussian-shaped EL bands. As an example, the EL spectral decomposition for sample 5a under the gate voltage of -15 V is shown in Fig. 5. As can be seen in this figure, the ~600-nm luminescence band dominates the EL spectrum with two shoulder bands centered at ~460 nm and ~740 nm. In addition, a luminescence band located at ~1260 nm was observed in the infrared region. Figure 6 shows the gate-voltage dependence of the contribution (in percentage) of each EL band for sample 5a. As can be seen in the figure, when the gate voltage increases, the contribution of the dominant EL band (i.e., the ~600-nm band) decreases, while the contribution of the ~460- and 740-nm band increase but the contribution of the ~1260-nm band shows no change.

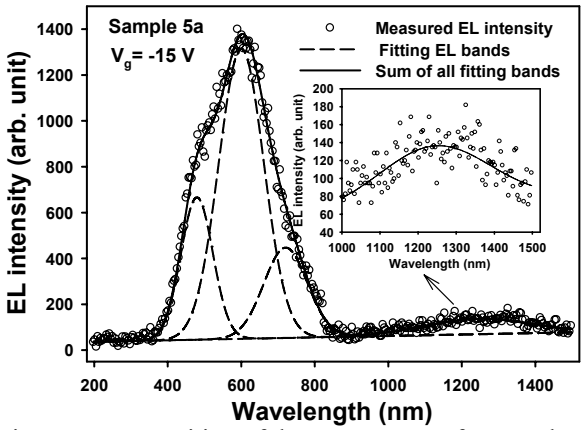

Fig. 5. Decomposition of the EL spectrum for sample 5a under the gate voltage of -15 V.

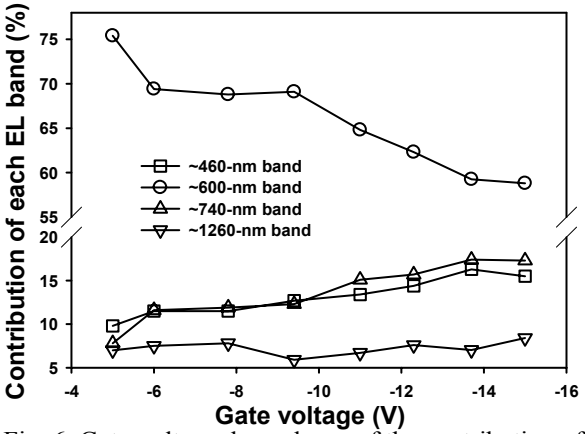

Fig. 6. Gate-voltage dependence of the contribution of each EL band for sample 5a.

Figure 7 shows the EL spectra for different samples under the gate voltage of -15 V. As shown in Fig. 9(a), it is found that a high implantation dose leads to an enhancement of the EL intensity for the sample with the implantation energy of 5 keV. This should be attributed to the higher efficiency of carrier injection for the samples fabricated with higher implanted Si ion dose, indicated by the fact that the gate current density increases with the Si ion dose, as shown in Fig. 3(a). Figure 7(b) shows the EL spectra for the sample fabricated under different implantation energy with the same Si ion dose (i.e., sample 8a, 5a, and 2a). It can be observed that the EL intensity increases with the implantation energy in the range of the study. This is also can be explained by the higher carrier injection for the sample fabricated with higher implantation energy, as suggested by the *I-V* characteristics shown in Fig. 3(b). For all the samples, the ~600-nm luminescence band dominates the EL spectra although the there are some variations in the contribution of each band. Figure 8 shows the contribution of each EL band under the gate voltage of -15 V for all the samples listed in Table 1. As shown in Fig. 8(a), the proportion of each EL band is almost independent of the Si ion dose. However, as shown in Fig. 10(b), when the implantation energy increase from 2 to 8 keV, the contribution of the ~600-nm band significantly increases from ~55% to ~61%, the contributions of both the ~740-nm and ~12600-nm band show almost no change, and the contribution of the ~460-nm EL band significantly decreases from 23% to 13%.

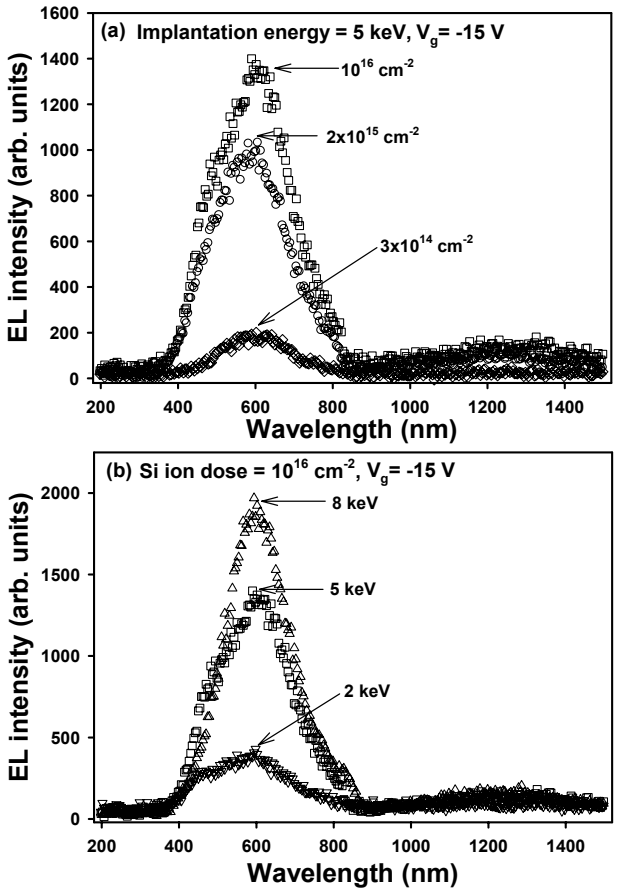

Fig. 7. (a) Influence of the implanted Si ion dose on the EL spectrum; (b) Influence of the implantation energy on the EL spectrum.

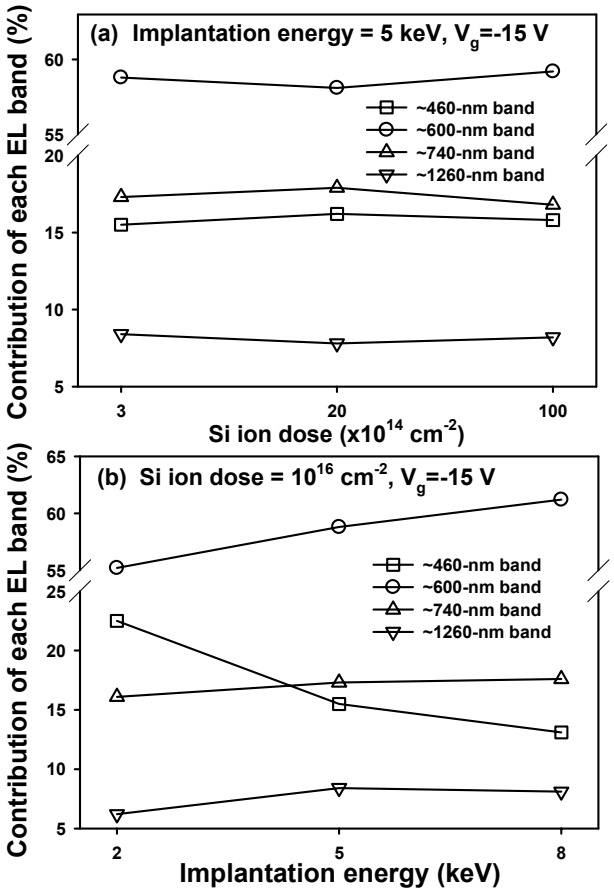

Fig. 8. (a) Contribution of each EL band as a function of the implanted Si ion dose; (b) Contribution of each EL band as a function of the implantation energy.

4. DISCUSSIONS

As well known, a high density of different kinds of point defects exist in most ion-implanted or radiation-damaged SiO_2 films. In previous studies, many kinds luminescent defects have been observed in the Si^+-implanted SiO_2 films, such as weak-oxygen bond (WOB) (O-O) defects, neutral oxygen vacancy (NOV) ($O_3 \equiv Si\text{-}Si \equiv O_3$), non-bridging oxygen hole center (NBOHC) ($O_3 \equiv Si\text{-}Si\text{-}O\bullet$), B_2 center, D center, and E' center.[10-18, 21-25] The experimental results obtained above

demonstrate that the EL spectra consist of the same four luminescence bands centered at ~460 , ~600, ~740, ~1260 nm for all the samples. Their origins may be attributed to the different radiative defects in SiO_2 film introduced by Si ion implantation or due to the existence of *nc*-Si. Under a negative gate voltage large enough, most electrons from the negatively biased ITO gate can tunnel through the SiO_2 into the conduction band of *p*-type Si substrate, and some electrons can be trapped by the higher energy levels of the defects in the SiO_2. The holes in *p*-type Si substrate can also be injected into the SiO_2 and be trapped by the ground states of the defects in the oxide. The radiative recombination of the trapped carriers at these occupied defect states in the SiO_2 should be responsible for the visible EL.

A blue luminescence band around 2.7 eV (~460 nm) has been reported from pure silica glass[34] and Si-rich silicon oxide[11, 13, 15, 16, 23] and has been ascribed to the neutral oxygen vacancies. This suggests that the NOV defects are the origin of the observed ~460-nm EL band. As reported by many researchers, the excitation of NOV defects as a luminescence center may be enhanced by the applied high electric filed in the oxide (E_{ox}) in the order of 10^6 V/cm.[16, 23, 34] This was indicated by the fact that the ~460-band proportion increases with the applied gate voltage, as shown in Fig. 8(b). In general, the gate voltage (V_g) is applied across the series combination of the junction at the ITO/oxide interface, the oxide film region, and the junction at oxide/Si interface as described by $V_g=V_1+V_2(E_{ox})+V_2$, where V_1, V_2, and V_3 are the voltage drops across the ITO/oxide junction, the oxide film region, and oxide/Si junction, respectively. Under the same gate voltage, it is obviously that there will be a higher electric filed E_{ox} in the oxide if the oxide resistance is higher, because V_g is mainly applied across the oxide region in this case. With this consideration, one may suppose that the contribution of ~460-nm band should increase with the oxide resistance under the same gate voltage. However, it is not the case presented in Fig. 8(a), which shows that the contribution of ~460-nm band does not increase with the decrease of Si ion dose (i. e., the increase in the oxide resistance). The stability should because that the number of NOV defects is reduced with the decrease of Si ion dose, and this compensates for the effect of increasing electric filed E_{ox} on the ~460-nm EL band proportion. For the study on the samples with the same Si ion dose which means the same number of NOV defects introduced, as shown in Fig. 8(b), the proportion of ~460-nm EL band decreases with the increasing of implantation energy, which lead to a decrease in the oxide resistance and thus a decrease in the electric filed E_{ox}. The results on the ~460-nm band evolution shown in Fig. 10 provide an indirect evidence that the ~460-nm originates from the NOV defects. It is known that the NBOHC defects in SiO_2 can emit light at around 2 eV.[16, 35] The domination of ~600-nm band in the EL spectra from the Si^+-implanted SiO_2 films was also reported by Song also.[16] This provides the possibility that can explain the origin of ~600-nm (~2 eV) luminescence band. In our experiments, the ~600-nm luminescence band always dominates the EL spectra for all the samples, indicating that the excitation energy of the ~600-nm band should be much lower than that of other luminescent defects and the energy distribution of injected carriers can easily satisfy the excitation of the NBOHC defects.

As regard to the ~740-nm (~1.7 eV) EL band, first we assume that it is probably due to the existence of *nc*-Si in the oxide, because there have not been any defects or interface states that can contribute to an emission band around 740nm in such an extensive literature. As mentioned above, the average diameter of *nc*-Si formed in the SiO_2 films in this study is ~4 nm. The ~740-nm photoluminescence band was observed which was believed to be due to the formation of *nc*-Si with a mean size of ~4 nm.[36] Thanks to many previous experimental [26, 27] and theoretical studies[37], the *nc*-Si with a diameter of ~4 nm was estimated to have a band gap of ~1.85 eV. The difference between the band gap and the emission energy indicates that the ~740-nm EL band should not originate from the direct band to band transition within the *nc*-Si. In fact, there are several studies that have demonstrated that the *nc*-Si with the size larger than ~1 nm still have an indirect band structure in both theoretical [38-40] and experimental aspects. [26, 40, 41] Therefore, the probability of direct band-to-band transition within the *nc*-Si is extremely low. It has been found that the energy difference (~0.15 eV) between the band gap and the emission energy is approximately equal to the energy (~0.134 eV) of Si-O vibration with a stretching frequency of 1083 cm^{-1}, implying the importance role of Si-O vibration at the *nc*-Si/SiO_2 interface in the 740-nm band luminescence. Considering the energy conservation and the indirect band structure of the *nc*-Si, we therefore are inclined to believe that the Si-O vibration at the *nc*-Si/SiO_2 interface provides the mean required for both the energy dissipation due to the energy conservation requirement and the momentum conservation in the EL process. In other words, the ~740-nm band can be attributed to the recombination of carries within the *nc*-Si assisted by the Si-O vibration at the *nc*-Si/SiO_2 interface.

As for the infrared EL band center at ~1260 nm, it mostly originates from the Si substrate. In order to confirm whether the virgin oxide and the substrate have any contribution to the observed EL spectra, we measured the EL spectra of the LEDs fabricated with pure thermal grown SiO_2 and SiO_2 films with different implanted elements, such as Ge and Al. Although the EL spectra in the visible range are different, all the samples exhibit infrared EL centered at ~1260 nm. The electrical driven infrared luminescence was also reported by Kulakci recently.[24] The light emission above 900 nm was

observed, although the authors could not determine the peak wavelength of the infrared EL due to the detector limitation. In our study, it is noticeable that the photon energy of peak infrared luminescence is ~0.985 V which has a difference of ~0.135 eV as compared with the band gap of bulk crystalline silicon. The energy difference is approximately the same with the Si-O vibration energy (0.134 eV). This observation makes us believe that the infrared EL band centered at ~1260 nm is a result of electron-hole recombination in the accumulation region formed beneath the oxide layer near the interface between the Si substrate and SiO_2. Such recombination is assisted by the Si-O bond with the vibration energy of ~0.134 eV at the Si/SiO_2 interface. In other words, the electron-hole recombination near the interface helps emit a photon with the energy of ~0.985 eV and a phonon of ~0.134 eV which is actually the Si-O vibration. This mechanism is similar that of the ~740-nm EL band, in which the energy and momentum compensation is provided by the Si-O vibration at the *nc*-Si/SiO_2 interface.

5. CONCLUSION

In summary, we have presented a systematic study on the EL properties of SiO_2 films embedded with *nc*-Si synthesized with low energy ion implantation. Light-emitting diodes are fabricated based on the ITO/SiO_2:Si^+/Al capacitor structure with various Si ion dose under different implantation energies. The current-voltage characteristics are investigated. It was found that gate current decreases with the reducing implantation energy and Si ion dose. The *I-V* characteristics are explained with the model of the tunneling path formed by neutral Si nanocrystals. Both visible and infrared electroluminescence has been observed. Four EL bands centered at ~460, ~600, ~740, and ~1260 nm are observed for all the samples. The first two EL bands are identified to be ascribed to the NOV and NBOHC defects, respectively. The ~740-nm band can be attributed to the recombination of carries within the *nc*-Si assisted by the Si-O vibration at the *nc*-Si/SiO_2 interface. The ~1260-nm EL band is assigned to originate from the electron-hole recombination in the accumulation region assisted by the Si-O vibration at interface between the SiO_2 and the Si substrate.

ACKNOWLEDGEMENT

This work has been financially supported by the Ministry of Education, Singapore, under project ARC No. 1/04 and the Singapore Millennium Foundation.

REFERENCES

[1] A. Liu, R. Jones, L . Liao, D. Samara-Rubio, D. Rubin, O. Cohen, R. Nicolaescu, and M. Paniccia, "A high-speed silicon optical modulator on a metal-oxide-semiconductor capacitor," Nature **427 (12)**, 615-618 (2004).

[2] A. Cutolo, M. Iodice, P. Spirito, and L. Zeni, "Silicon electro-optic modulator based on a three terminal device integrated in a low-loss single-mode SOI waveguide," J. Lightwave Technol. **15(3)**, 505-518 (1997).

[3] Y. Liu, E. Liu, G. Li, S. Zhang, J. Luo, F. Zhou, M. Cheng, B. Li, and H. Ge, "Novel silicon waveguide switch based on total internal reflection," Appl. Phys. Lett. **64(16)**, 2079-2081 (1994).

[4] C. Z. Zhao, A. H. Chen, E. K. Liu, and G. Z. Li, "Silicon-on insulator asymmetric optical switch based on total internal reflection," IEEE Photon. Technol. Lett. **9(8)**, 1113-1115 (1997).

[5] R. A. Soref, F. Namavar, N. M. Kalkhoran, and D. M. Koker, "Silicon optical waveguides with buried-$CoSi_2$ cladding layers," Opt. Lett. **19(17)**, 1319-1321 (1994).

[6] H. Rong, A. Liu, R. Nicolaescu, M. Paniccia, O. Cohen, and D. Hak, "Raman gain and nonlinear optical absorption measurements in low-loss silicon waveguide," Appl. Phys. Lett. **85(12)**, 2196-2198 (2004).

[7] M. Ghioni, F. Zappa, V. P. Kesan, and J. Warnock, "A VLSI-compatible high-speed silicon photodetector for optical data link applications," IEEE Trans. Electron Devices **43(7)**, 1054-1060 (1996).

[8] A. R. Hawkins, W. Wu, P. Abraham, K. Streubel, and J. E. Bowers, "High gain-bandwidth-product silicon heterointerface photodetector," Appl. Phys. Lett. **70(3)**, 303-305 (1997).

[9] L. T. Canham, "Silicon quantum wire array fabrication by electrochemical and chemical dissolution of wafers," Appl. Phys. Lett. **57(10)**, 1046-1048 (1990).

[10] T. Shimizu-Iwayama, K. Fujita, S. Nakao, K. Saitoh, T. Fujita, and N. Itoh, "Visible photoluminescence in Si^+-implanted silica glass," J. Appl. Phys. **75(12)**, 7779-7783 (1994).

[11] H. Nishikawa, E.Watanabe, D. Ito, M. Takiyama, A. Leki, and Y. Ohki, "Photoluminescence study of defects in ion-implanted thermal SiO_2 films," J. Appl. Phys. **78(2)**, 842-846 (1995).

[12] P. Mutti, G. Ghislotti, S. Bertoni, L. Bonoldi, G. F. Cerofolini, L. Meda, E. Grilli, and M. Guzzi, "Room-temperature visible luminescence from silicon nanocrystals in silicon implanted SiO_2 layers," Appl. Phys. Lett. **66(7)**, 851-853 (1995).
[13] L. S. Liao, X. M. Bao, X. Q. Zheng, N. S. Li, and N. B. Min, "Blue luminescence from Si^+-implanted SiO_2 films thermally grown on crystalline silicon," Appl. Phys. Lett. **68(6)**, 850-852 (1996).
[14] W. Skorupa, R. A. Yankov, I. E. Tyschenko, H. Frob, T. Bohme, and K. Leo, "Room-temperature, short-wavelength (400-500 nm) photoluminescence from silicon-implanted silicon dioxide films," Appl. Phys. Lett. **68(17)**, 2410-2412 (1996).
[15] H.-Z. Song and X.-M. Bao, "Visible photoluminescence from silicon-ion-implanted SiO_2 film and its multiple mechanisms," Phys. Rev. B **55(11)**, 6988-6993 (1997).
[16] H.-Z. Song, X.-M. Bao, N.-S. Li, and J.-Y. Zhang, "Relation between electroluminescence and photoluminescence of Si^+-implanted SiO_2," J. Appl. Phys. **82(8)**, 4028-4032 (1997).
[17] L. Rebohle, J. von Borany, R. A. Yankov, W. Skorupa, I. E. Tyschenko, H. Frob, and K. Leo, "Strong blue and violet photoluminescence and electroluminescence from germanium-implanted and silicon-implanted silicon-dioxide layers," Appl. Phys. Lett. **71(19)**, 2809-2811 (1997).
[18] K. Luterova, I. Pelant, J. Valenta, J.-L. Rehspringer, D. Muller, J. J. Grob, and J. Dian, "Red luminescence in Si^+-implanted sol-gel-derived SiO_2 films," Appl. Phys. Lett. **77(19)**, 2952-2954 (2000).
[19] Y. Liu, T. P. Chen, Y. Q. Fu, M. S. Tse, J. H. Hsieh, P. F. Ho, Y. C. Liu, "A study on Si nanocrystal formation in Si-implanted SiO_2 films by x-ray photoelectron spectroscopy," J. Phys. D: Appl. Phys **36**, L97-L100 (2003).
[20] T. P. Chen, Y. Liu, C. Q. Sun, M. S. Tse, J. H. Hsieh, Y. Q. Fu, Y. C. Liu, and S. Fung, "Core-level shift of Si nanocrystals embedded in a SiO_2 matrix," J. Phys. Chem. B. **108(43)**, 16609-16612 (2004).
[21] A. Pèrez-Rodrìguez, O. González-Varona, B. Garrido, P. Pellegrino, J. R. Morante, C. Bonafos, M. Carrada, and A. Claverie, "White luminescence from Si and C ion-implanted SiO_2 films," J. Appl. Phys. **94(1)**, 254-261 (2003).
[22] T. Matsuda, K. Nishihara, M. Kawabe, H. Iwata, S. Iwatsubo, and T, Ohzone, "Blue electroluminescence from MOS capacitors with Si-implanted SiO_2," Solid-State Electron. **48(10)**, 1933-1941 (2004).
[23] Chun-Jung Lin and Gong-Ru Lin, "Defect-enhanced visible electroluminescence of multi-energy silicon implanted silicon dioxide film," IEEE J. Quantum Electron. **41(3)**, 441-447 (2005).
[24] M. Kulakci, U. Serincan, and R. Turan, "Electroluminescence generated by a metal oxide semiconductor light emitting diode (MOS-LED) with Si nanocrystals embedded in SiO_2 layers by ion implantation," Semicond. Sci. Technol. **21,** 1527-1532 (2006).
[25] L. Ding, T. P. Chen, Y. Liu, C. Y. Ng, and S. Fung, "Optical properties of silicon nanocrystals embedded in a SiO_2 matrix," Phys. Rev. B **72(12)**, 125419-1–125419-7 (2005).
[26] L. Ding, T. P. Chen, Y. Liu, C. Y. Ng, Y. C. Liu, and S. Fung, "Thermal annealing effect on the band gap and dielectric functions of silicon nanocrystals embedded in SiO_2 matrix," Appl. Phys. Lett. **87(12)**, 121903-1–121903-3 (2005).
[27] C. Y. Ng, T. P. Chen, L .Ding, M. Yang, J. I. Wong, P. Zhao, X. H. Yang, K. Y. Liu, M. S. Tse, A. D. Trigg, and S. Fung, "Influence of Si nanocrystal distributed in the gate oxide on the MOS capacitance," IEEE Trans. Electron Devices **53(4)**, 730-736 (2006).
[28] C. Y. Ng, T. P. Chen, L .Ding, Q. Chen, Y. Liu, P. Zhao, Ampere A. Tseng, and S. Fung, "Si ion-induced instability in flatband voltage of Si^+-implanted gate oxides," IEEE Trans. Electron Devices **53(5)**, 1281-1282 (2006).
[29] L. Ding, T. P. Chen, J. I. Wong, M. Yang, Y. Liu, C. Y. Ng, Y. C. Liu, C. H. Tung, A. D. Trigg, and S. Fung, "Dielectric function of densely stacked Si nanocrystal layer embedded in SiO_2 thin films," Appl. Phys. Lett. **89(25)**, 251910-1–251910-3 (2006).
[30] K. Zhang, F. Zhu, C. H. A. Huan, and A. T. S. Wee, "Effect of hydrogen partial pressure on optoelectronic properties of indium tin oxide thin films deposited by radio frequency magnetron sputtering method," J. Appl. Phys. **86(2)**, 974-980 (1999).
[31] J. Hu, J. Pan, F. Zhu, and H. Gao, "Evidence of nitric-oxide-induced surface band bending of indium tin oxide," J. Appl. Phys. 95(11), 6273-6276 (2004).
[32] Y. Li, L.-W. Tan, X.-T. Hao, K. S. Ong, F. Zhu, and L.-S. Hung, "Flexible top-emitting electroluminescent devices on polyethylene terephthalate substrates," Appl. Phys. Lett. **86(15)**, 153508-1–153508-3 (2005).
[33] Y. Liu, T. P. Chen, C. Y. Ng, M. S. Tse, S, Fung, Y. C. Liu, S. Li, and P. Zhao, "Charging effect on electrical characteristics of MOS structures with Si nanocrystal distribution in gate oxide," Electrochem. Solid-State Lett. **7(7)**, G134–G137 (2004).

[34] R. Tohmon, Y. Shimogaichi, H. Mizuno, and Y. Ohki, "2.7-eV luminescence in as-manufactured high-purity silicon glass," Phys. Rev. Lett. **62(12)**, 1388-1391 (1989).
[35] L. Skuja, "Time-resolved temperature luminescence of non-bridging oxygen hole centers in silicon glass," Solid State Commun. **84(6)**, 613-616 (1992).
[36] M. Y. Valakh, V. A. Yukhimchuk, V. Y. Bratus, A. A. Konchits, P. L. F. Hemment, and Komoda, "Optical and electron paramagnetic resonance study of light-emitting Si^+-ion implanted silicon dioxide layers," J. Appl. Phys. **85(1)**, 168-173 (1999).
[37] S. Ogut, J. R. Chelikowsky, and S. G. Louie, "Quantum confinement and optical gaps in Si nanocrystals," Phys. Rev. Lett. **79(9)**, 1770-1773 (1997).
[38] G. Allan, C. Delerue, and M. Lannoo, "Nature of luminescent surface states of semiconductor nanocrystals," *Phys. Rev. Lett.*, vol. 76, no, 16, pp. 2961–2964, Apr. 1996.
[39] M. H. Nayfeh, N. Rigakis, and Z, Yamani, "Photoexcitation of Si-Si surface states in nanocrsytallites," Phys. Rev. B **56(4)**, 2079-2084 (1997).
[40] M. S. Hybertsen, "Absorption and emission of light in nanoscale silicon structures," Phys. Rev. Lett. **72(10)**, 1514-1517 (1994).
[41] D. Kovalev, J. Diener, H. Heckler, G. Polisski, N. Kunzner, and F. Koch, "Optical absorption cross section of Si nanocrystals," Phys. Rev. B **61**(7), 4485-4487 (2000).